IEEE Access
Multidisciplinary | Rapid Review | Open Access Journal

Received May 3, 2020, accepted May 23, 2020, date of publication May 26, 2020, date of current version June 30, 2020.

Digital Object Identifier 10.1109/ACCESS.2020.2997825

Distributed Sensor Management Based on Target Losing Probability for Maneuvering Multi-Target Tracking

GANLIN SHAN AND CE PANG
Shijiazhuang Campus of Army Engineering University, Shijiazhuang 050003, China

Corresponding author: Ce Pang (guanglongzhu@163.com)

This work was supported in part by the Defense Pre-Research Fund Project of China (DPRFC) under Grant 012015012600A2203, and in part by the Natural Science Foundation of China (NSFC) under Grant 61573374.

ABSTRACT This paper proposed a distributed sensor management method in the constraint of target losing probability for maneuvering multi-target tracking. Three main contributions existed in this paper, including adding the emission interception risk to the sensor management objective function, analyzing actual working modes of radars and regarding the target losing probability as one of constraints in sensor management. Two kind of radar working modes were introduced. They were the single target tracking mode and the multiple target tracking mode, leading to different kinds of sensor management methods. Then two sensor management models, containing sensor management in a large defending scope and in a small defending scope, were built. After that, the distributed sensor management process was introduced. Finally, simulations were conducted to show the effectiveness and efficiency of the proposed sensor management methods. By applying the proposed sensor management method, targets couldn't be easily lost and radar could be well protected at the same time.

INDEX TERMS Sensor management, target tracking, distributed sensor networks, target losing probability.

I. INTRODUCTION

Sensor networks, especially radar networks, are usually used to detect targets in military. They should be managed or scheduled in a proper way to behave a perfect sensing performance. It is a better way to make full use of sensor resources through sensor management, and this topic has been a hot and attracted researches all over the world for many years. In sensor management, there are formally two steps. An objective function should be established firstly and after that, the optimal sensor management schemes should be calculated. The calculated sensor management scheme is carried out to get observations, which will be used to estimate motion states of targets [1]–[4].

Sensor management can be divided into two categories, including immobile sensor management and mobile sensor management. For immobile sensors, their locations are unchanged and stable. And in immobile sensor management, one sensor is usually assumed to track only one target. Sensors are allocated to targets in a proper way to maximize the efficiency of sensor networks [5]–[8]. The main research in this aspect is how to calculate the best sensor-target allocation scheme. However, in mobile sensor management, sensors can adjust their locations to improve their tracking performance [9]–[12]. And in this aspect, optimizing the motion trajectory of sensors is the main work.

For the both two categories of sensor management, the method of building the objective function in sensor management can be concluded as follows [13], [14].

The first category is the sensor management method based on covariance [15]–[18]. In this method, the target tracking accuracy is defined based on error covariance matrix firstly. And when managing sensors, the target tracking accuracy is optimized as the objective function or satisfied as one of the constraints. The second category is the information based sensor management method [19]–[23]. In this method, the information gain obtained by observations is maximized in sensor management. This method has been proved to be the same principle as the former sensor management method with the same optimal solution obtained. The third one is

The associate editor coordinating the review of this manuscript and approving it for publication was Sanket Goel.

the sensor management method based on random sets for multi-objective tracking [24]–[27]. The difference between this method and the former two kinds of methods is mainly on the target tracking theory, rather than the optimization principle. The fourth kind of sensor management methods is based on optimization algorithm, including centralized algorithm and distributed algorithm. In sensor management method based on centralized algorithm, there are sensor management methods based on the planning theory [28], [29] and intelligent algorithm [30], [31]. In distributed algorithm, the sensor management method is mainly based on game theory [32], [33]. In this aspect, the optimization process can be seen as the multiple sensor gaming process obeying the biggest local optimization.

Sensors are radars in this paper. Although sensor management methods mentioned above can achieve pretty perfect target tracking performance, for example, satisfying tracking accuracy, three main issues existing in the former researches mentioned above.

Firstly, the mentioned references have seldom taken the emission interception probability into consideration. That is to say, the safety of radars have been ignored in the former researches. Nowadays, anti-radiation weapons have been developed rapidly. When radars are tracking targets, the safety of them is also threatened. The emission interception should not be ignored for that targets can intercept our emission to find positions of sensors and they can further launch missiles to destroy our sensors. In another word, in the process of emitting radiations, the safety of radars should also be taken into consideration firstly.

Secondly, working modes of sensors are often not taken into consideration. However, different kinds of radar working modes need different kinds of sensor management methods. The former researches has not discussed the application scope and limitation of existing sensor management methods. There are two working modes of radars. The first one is taking measurements by focusing one radar beam on one target's position, resulting that one radar can only track one target mostly with a bigger emission interception probability and a better tracking accuracy. The other one is to scan all directions using one radar beam at the same time, leading to the fact that one radar can track multiple targets contemporary with a less emission interception probability and a worse tracking accuracy. Obviously, different working modes of radars result in different target tracking performance. In the first working mode, the sensor management can be seen as the sensor-target allocation problem, which has been analyzed in the former researches. However, in the multiple target tracking mode, the sensor-target tracking allocation is meaningless. But in this mode, sensors can adjust their positions to improve tracking performance. And this is the second sensor management problem. There is rarely related researches. Analyzing the impact of radars' working modes on the target tracking performance is also an important job in this paper.

The last but not the least is that the former references often improve the tracking performance as much as possible, ignoring the combat requirement. If the combat order is just to track targets in order to keep them not lost, but not to destroy them, we needn't consume much radar resources to keep a high tracking accuracy, leading to a high emission interception probability. The former researches hold the point that a sensor management method with better tracking performance is better. For example, they think the more accurate one sensor management scheme has, the more perfect the sensor management scheme is. Obviously, this is not suitable for the case mentioned above.

In order to solve the problems mentioned above, this paper mainly focuses on the following points.

Firstly, we try to reduce the emission in case of interception on the condition that the tracking accuracy is satisfied. Only by doing so, the safety of radars can be ensured. Then target can be tracked perfectly. In sensor management, on one hand, the radar emission interception probability will be reduced. On the other hand, the target tracking accuracy will be improved. The two aspects are combined in the objective function of sensor management.

Secondly, different form the former researches, the working modes of radars will be introduced and analyzed. The two kinds of related sensor management methods will be proposed. In the single target tracking mode, the sensor-target allocation schemes will be optimized. This case can be applied to target tracking in a large scope. In the multiple target tracking mode, the motion trajectories of sensors will be optimized. This case can be used to target tracking in a small scope. All in all, sensor management method proposed in this paper can solve both the two kinds of sensor management problems.

Thirdly, we add the target losing probability to the constraints of the sensor management objective function in case of radar resource wasting. We take the target tracking case, where target can be kept just not lost and not escape from our monitoring scope, into consideration. In this case, improving the target tracking accuracy as much as possible will lead to sensor resource wasting. On another hand, this point can effectively reduce the sensor emission and keep radar in a low emission level.

Sensors are scheduled in the distributed network. When producing sensor management orders, we just use the greedy algorithm to solve the objective function to produce sensor management schemes. The emphasis of this paper is not the optimization algorithm.

Based on the analysis above, this paper proposes a sensor management method in the constraint of target losing probability for maneuvering multi-target tracking. The rest of this paper is organized as follows. Section II introduces the basic knowledge of target tracking, including the maneuvering target moving model, measurement model, the two working modes of radars, and the methods of estimating target motion state. In section III, the target losing probability is analyzed and its calculation method is proposed. In section IV, two sensor management models, containing sensor management in a large defending scope and sensor management in a small defending scope, are built after the calculation of the radar emission interception probability is proposed. What's more, the distributed sensor management process is also described. Some simulations are made in section V to illustrate the effectiveness of the method and algorithm in this paper before section VI concludes the paper.

II. PRELIMINARIES

A. THE MANEUVERING TARGET MOVING MODEL AND MEASUREMENT MODEL

Two moving modes are combined and taken into consideration, including a constant velocity (CV) mode and a coordinated turning (CT) mode. When targets are moving, the two moving modes can be converted to the other one randomly.

In a two-dimensional Cartesian space, the motion state of a target is noted as $\boldsymbol{x}(k) = [x(k), \dot{x}(k), y(k), \dot{y}(k), \Omega(k)]^T$ at time instant k, evolving as the following equation:

$$\boldsymbol{x}(k|k-1) = f\left(\boldsymbol{x}(k-1)\right) + \boldsymbol{w}(k-1) \tag{1}$$

where there are the variable

$$\frac{\partial f}{\partial \boldsymbol{x}} = \mathbf{F}(\boldsymbol{k}) = \begin{bmatrix} 1 & \Delta T & 0 & 0 & 0 \\ 0 & 1 & 0 & 0 & 0 \\ 0 & 0 & 1 & \Delta T & 0 \\ 0 & 0 & 0 & 1 & 0 \\ 0 & 0 & 0 & 0 & 1 \end{bmatrix}$$

and $\Omega(k) = 0$ when the target is moving with a constant velocity(CV), and there is the variable

$$\frac{\partial f}{\partial \boldsymbol{x}} = \mathbf{F}(k) = \begin{bmatrix} 1 & \dfrac{\sin\Omega(k)T}{\Omega(k)} & 0 & -\dfrac{1-\sin\Omega(k)T}{\Omega(k)} & 0 \\ 0 & \cos\Omega(k)T & 0 & -\sin\Omega(k)T & 0 \\ 0 & \dfrac{1-\cos\Omega(k)T}{\Omega(k)} & 1 & \dfrac{\sin\Omega(k)T}{\Omega(k)} & 0 \\ 0 & \sin\Omega(k)T & 0 & \cos\Omega(k)T & 0 \\ 0 & 0 & 0 & 0 & 1 \end{bmatrix}$$

when the target is in a coordinated turning (CT) mode; The variable $\boldsymbol{w}(k-1)$ is a process noise, which obeys the distribution $p(\boldsymbol{w}) - N(0, \mathbf{Q})$, and there is

$$\mathbf{Q} = \sigma_\omega^2 \begin{bmatrix} 1/3\Delta T^2 & 1/2\Delta T^2 & 0 & 0 & 0 \\ 1/2\Delta T^2 & \Delta T & 0 & 0 & 0 \\ 0 & 0 & 1/3\Delta T^2 & 1/2\Delta T^2 & 0 \\ 0 & 0 & 1/2\Delta T^2 & \Delta T & 0 \\ 0 & 0 & 0 & 0 & \Delta T \end{bmatrix}.$$

Sensors are radars in this paper. There are M radars in the distributed radar network, which are denoted as $\{s_1, s_2, \ldots, s_i, \ldots, s_M\}$.

An observation from radars s_i is shown as follows.

$$\begin{cases} z_i(k) = \boldsymbol{h}_i(x(k), x_i^s) + \boldsymbol{v}_i(k) \\ \boldsymbol{h}_i(x(k), x_i^s) \\ = [r_i(k), \theta_i(k)]^T \\ = \begin{bmatrix} \sqrt{(x(k) - x_i^s(k))^2 + (y(k) - y_i^s(k))^2}, \\ \arctan\left(\dfrac{y(k) - y_i^s(k)}{x(k) - x_i^s(k)}\right) \end{bmatrix} \end{cases} \tag{2}$$

where the variable $v_i(k)$ denotes a measurement noise with the distribution $p(v) - N(\mathbf{0}, \mathbf{R}_i(k))$, and covariance matrix $\mathbf{R}_i(k) = diag\left[\sigma_{r_i}^2(k), \sigma_{\theta_i}^2(k)\right]$; The variable $(x_i^s(k), y_i^s(k))$ is the coordination of radar s_i at time instant k.

After linearization, there is

$$\boldsymbol{H} = \frac{\partial \boldsymbol{h}}{\partial \boldsymbol{x}} = \begin{bmatrix} \dfrac{\Delta x_i}{r_i} & 0 & \dfrac{\Delta y_i}{r_i} & 0 \\ -\dfrac{\Delta y_i}{r_i^2} & 0 & \dfrac{\Delta x}{r_i^2} & 0 \end{bmatrix},$$

where there is $\Delta x_i = x(k|k-1) - x_i^s$, $\Delta y_i = y(k|k-1) - y_i^s$, and $r_i = \sqrt{(\Delta x_i)^2 + (\Delta y_i)^2}$. The covariance matrix of measurement noise changes with the radiation time and the distance between targets and radars as follows [34].

$$\begin{cases} \sigma_{r_i}(k) = \sigma_{r,cal}\sqrt{(SNR_i(k)/SNR_{cal})} \\ \sigma_{\theta_i}(k) = \sigma_{\theta,cal}\sqrt{(SNR_i(k)/SNR_{cal})} \\ SNR_{0i}(k) = SNR_{cal}\left(\dfrac{\tau}{\tau_{cal}}\right)\left(\dfrac{d}{d_{cal}}\right)^{-4} \\ SNR_i(k) = SNR_{0i}(k)\exp\left(-4\ln(2)\dfrac{\tilde{a}^2}{B^2}\right) \end{cases} \tag{3}$$

where the variable $SNR_{cal} = 12$, $\sigma_{r,cal} = 200m$, $\sigma_{\theta,cal} = 0.1rad$, $\tau_{cal} = 10ms$ and $d_{cal} = 40km$ are calibrated values; The variable $B = 3dB$ is a half power width; The variable $\tilde{a}$ denotes the mismatch between the direction of one radar beam and the actual target azimuth.

It can be seen that with the distance of the target and the sensor changing, the three values, SNR, $\sigma_{r_i}(k)$ and $\sigma_{\theta_i}(k)$ are all changing, not keeping stable. The target detection probability $p_d(k)$ can be calculated by [35]:

$$\begin{cases} p_d = 0.5\operatorname{erfc}(\sqrt{-\ln p_{fa}} - \sqrt{SNR + 0.5}) \\ \operatorname{erfc}(z) = 1 - \dfrac{2}{\sqrt{\pi}}\displaystyle\int_0^z e^{-v^2}dv \end{cases} \tag{4}$$

where the variable p_{fa} is the false alarming probability.

When there are $m(k)$ sensors tracking the same target at the same time, the joint detection probability can be calculated by the following equation.

$$p_d^*(k) = 1 - \prod_{i=1}^{m_k}\left(1 - p_d^i(k)\right) \tag{5}$$

where the variable $p_d^i(k)$ is the detection probability.

Example 1: Suppose that the coordinate of a sensor is $s_i(0, 5)$, the original position of target is (0,50), its velocity is (1,−1), and there is $\tilde{a} = 0$. The radiation time of one observation is $\tau = 10ms$. There is $p_{fa} = 0.01$. The unit of variables is km. When target is moving in 50 seconds, changes of SNR, $\sigma_{r_i}(k)$, $\sigma_{\theta_i}(k)$ and $p_d(k)$ are in Fig.1.

The tracking performance varies when the target moves. It can be seen from Fig.1 (c) and (f) that if the value of SNR is big enough, the target detection probability can be "1", that is to say, in this case, the target must be found.

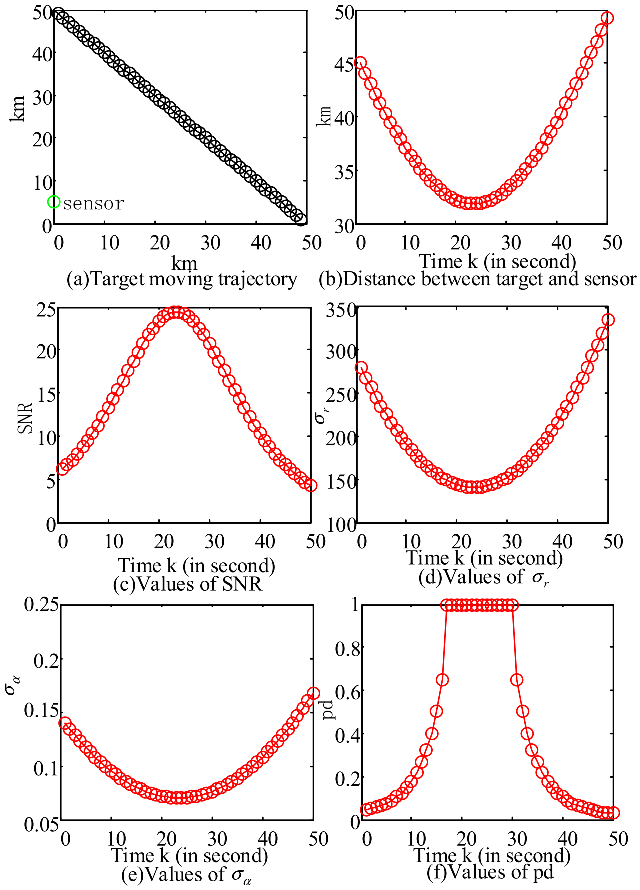

FIGURE 1. Changes of SNR, $\sigma_{r_i}(k)$, $\sigma_{\theta_i}(k)$ and $p_d(k)$ when the target moves.

The values of SNR and p_d are inversely proportional to the distance between the target and the sensor. The values of σ_{r_i} and σ_{θ_i} are proportional to the distance.

B. METHODS OF ESTIMATING TARGETS' MOTION STATE

There are two working modes in radars, and they are tracking one special target using its one beam (working mode 1) and tracking multiple targets by scanning all monitoring space (working mode 2) in one observation period as Fig.2 shows.

The tracking accuracy of the first one outperforms the second one for the reason that its beam dwelling time in one target is longer with the same radiation power and emission time. However, in the second working mode, one radar can keep tracking multiple targets at the same time.

Some assumptions are proposed in this paper as follows.

Assumption 1: The number of targets keeps not changeable in the whole target tracking process. Targets can't occur or disappear suddenly;

Assumption 2: Each radar has two working modes mentioned above, so as to track a single target or track multiple targets at the same time. Due to this case, in the far distance between targets and radars, single target tracking mode is taken, and in the near distance, multiple target tracking mode

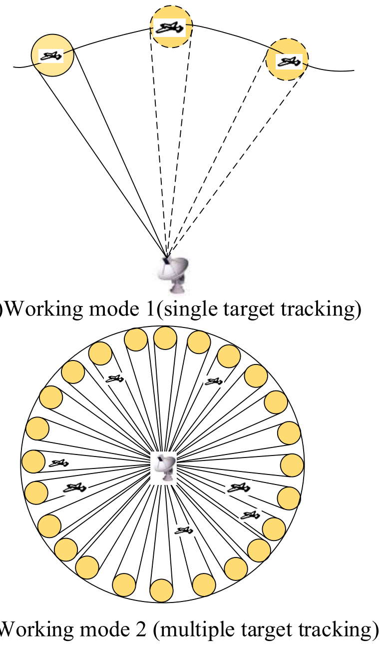

FIGURE 2. Radar's two kinds of working modes.

is taken. Different working modes result in different sensor management methods;

Assumption 3: For each radar, its radiation power and time in one period of observation keeps unchangeable;

Assumption 4: The time interval ΔT is unchangeable;

Assumption 5: Each sensor can only produce one observation from one target at most, and one observation is allocated to one target at most;

Assumption 6: This paper studies the problem of sparse target tracking.

Assumption 7: Each radar keeps its emission time, power, and beam width unchangeable. That is to say, in the multiple target tracking mode, the emission time can be seen equal to $\tau' = \tau\theta/360$, where the variable θ is the width of the radar beam.

1) SINGLE TARGET TRACKING ALGORITHM BASED ON IMM

In the single target tracking mode, IMM is used to estimate the states of maneuvering targets. The calculation process is shown in Table 1 in the appendix. At time instant k, the input of IMM is the target motion states $(\hat{\boldsymbol{x}}(k-1|k-1), \hat{\boldsymbol{P}}(k-1|k-1))$ and observations $\boldsymbol{z}(k)$, and the output is the target motion states $(\hat{\boldsymbol{x}}(k|k), \hat{\boldsymbol{P}}(k|k))$.

2) MULTI-TARGET TRACKING ALGORITHM BASED ON DATA ASSOCIATION ALGORITHM

In this case, one radar is assumed to be able to maintain tracking multiple targets at the same, which means that it can obtain observations of all targets simultaneously.

After a sensor has obtained multiple observations from targets meanwhile, observations should be associated to targets respectively. Dada association algorithm should be applied to

TABLE 1. **Algorithm 1: IMM algorithm.**

Algorithm initialization:

At time instant k, the target motion state of time instant $k-1$ is $\hat{\boldsymbol{x}}(k-1|k-1)$, with the covariance matrix $\hat{\boldsymbol{P}}(k-1|k-1)$. The variable g denotes the number of target moving model. The motion model probability matrix is $\boldsymbol{u}(k-1)_{g\times 1}$. The state transmission matrix of models is $\Pi=\left[\pi_{ij}\right]_{g\times g}$, where the viable π_{ij} denotes the probability of translating from model i to model j, and there is $\sum_{j=1}^{g}\pi_{ij}=1$ obviously.

Step 1: Input the initial interaction.

The initial interaction is as follows.

$$c^{j}(k-1)=\sum_{i=1}^{g}\pi_{ij}\mu^{i}(k-1),\ \mu^{ij}(k-1)=\frac{1}{c^{j}(k-1)}\pi_{ij}\mu^{i}(k-1) \tag{19}$$

where the variable $c^{j}(k-1)$ is the existing probability of model j after interaction; The variable $\mu^{i}(k-1)\in\boldsymbol{u}(k-1)_{g\times 1}$ denotes the existing probability of model i at time instant $k-1$; The variable $\mu^{ij}(k-1)$ denotes the existing probability of model j translating from model i after normalization.

Relatively, the initial state after inputting interaction $\hat{\boldsymbol{x}}^{0j}(k-1|k-1)$ and covariance matrix $\hat{\boldsymbol{P}}^{0j}(k-1|k-1)$ are as follows.

$$\begin{cases}\hat{\boldsymbol{x}}^{0j}(k-1|k-1)=\sum_{i=1}^{g}\hat{\boldsymbol{x}}^{i}(k-1|k-1)u^{ij}(k-1)\\ \hat{\boldsymbol{P}}^{0j}(k-1|k-1)=\sum_{i=1}^{g}\begin{bmatrix}\hat{\boldsymbol{P}}^{i}(k-1|k-1)+\left(\hat{\boldsymbol{x}}^{i}(k-1|k-1)-\hat{\boldsymbol{x}}^{0j}(k-1|k-1)\right)\\ \left(\hat{\boldsymbol{x}}^{i}(k-1|k-1)-\hat{\boldsymbol{x}}^{0j}(k-1|k-1)\right)^{T}\end{bmatrix}u^{ij}(k-1)\end{cases} \tag{20}$$

where the variables $\hat{\boldsymbol{x}}^{0j}(k-1)$ and $\hat{\boldsymbol{P}}^{0j}(k-1)$ denote the estimation of motion states and covariance matrix after interaction.

Step 2: Estimate the states of all motion models based on EKF.

Estimate the motion states of all motion models. The filtering based on EKF is as follows.

$$\begin{cases}\bar{\boldsymbol{x}}^{j}(k|k-1)=\boldsymbol{F}^{j}(k-1)\hat{\boldsymbol{x}}^{0j}(k-1|k-1),\bar{\boldsymbol{P}}^{j}(k|k-1)\\ =\boldsymbol{F}^{j}(k-1)\hat{\boldsymbol{P}}^{0j}(k-1|k-1)\boldsymbol{F}^{j}(k-1)^{T}+\boldsymbol{Q}_{k}\\ \boldsymbol{S}^{j}(k)=\boldsymbol{H}(k)\bar{\boldsymbol{P}}^{j}(k|k-1)\boldsymbol{H}^{T}(k)+\boldsymbol{R}(k),\boldsymbol{K}^{j}(k)\\ =\bar{\boldsymbol{P}}^{j}(k|k-1)\boldsymbol{H}^{T}(k)\left(\boldsymbol{S}^{j}(k)\right)^{-1}(k)\\ \hat{\boldsymbol{x}}^{j}(k|k)=\bar{\boldsymbol{x}}^{j}(k|k-1)+\boldsymbol{K}^{j}(k)(\boldsymbol{Y}(k)-\boldsymbol{h}(\bar{\boldsymbol{x}}^{j}(k|k-1)))\\ \hat{\boldsymbol{P}}^{j}(k|k)=(\boldsymbol{I}-\boldsymbol{K}^{j}(k)\boldsymbol{H}(k))\bar{\boldsymbol{P}}^{j}(k|k-1)\end{cases} \tag{21}$$

where the variable $\boldsymbol{F}$ is the state transmission matrix; $\boldsymbol{Q}$ and $\boldsymbol{R}$ are the noise matrix; $\boldsymbol{K}$ is the information gain matrix; $\boldsymbol{I}$ is the unit matrix; $\boldsymbol{h}$ is the observation matrix; $\boldsymbol{Y}$ is the observation.

Step 3: Update the existing probability of all motion models.

The likelihood function of motion models can be calculated by:

$$\Delta^{j}(k)=\frac{1}{\sqrt{(2\pi)^{\mathrm{M}}\left|\boldsymbol{S}^{j}(k)\right|}}\exp\left(-\frac{\begin{pmatrix}\left(z(k)-\boldsymbol{H}(k)\bar{\boldsymbol{x}}^{j}(k|k-1)\right)^{T}\boldsymbol{S}^{j}(k)\\ \left(z(k)-\boldsymbol{H}(k)\bar{\boldsymbol{x}}^{j}(k|k-1)\right)\end{pmatrix}^{-1}}{2}\right) \tag{22}$$

where the variable M is the dimension of measurement.

The existing probability of motion models can be updated by:

$$\mu^{j}(k)=\Delta^{j}(k)c^{j}(k-1)/C(k),C(k)=\sum_{i=1}^{g}\Delta^{j}(k)c^{j}(k-1) \tag{23}$$

TABLE 1. ***(Continued)*** **Algorithm 1: IMM algorithm.**

Step 4: Sum the filtering results.

The motion state and covariance of the target can be summed as the following equations.

$$\begin{cases}\hat{\boldsymbol{x}}(k|k)=\sum_{j=1}^{g}\hat{\boldsymbol{x}}^{j}(k|k)u^{j}(k)\\ \hat{\boldsymbol{P}}(k|k)=\sum_{j=1}^{g}\left[\hat{\boldsymbol{P}}^{j}(k|k)+\left(\hat{\boldsymbol{x}}^{j}(k|k)-\hat{\boldsymbol{x}}(k|k)\right)\left(\hat{\boldsymbol{x}}^{j}(k|k)-\hat{\boldsymbol{x}}(k|k)\right)^{T}\right]u^{j}(k)\end{cases} \tag{24}$$

Step 5: Fuse the results from different radars.

If there are $m(k)$ radars are tracking one target at the same time, the fusion results can be calculated as follows.

$$\begin{cases}\hat{\boldsymbol{x}}^{*}(k|k)=\sum_{h=1}^{m(k)}\hat{\boldsymbol{x}}^{h}(k|k)\\ \hat{\boldsymbol{P}}^{*}(k|k)=\sum_{h=1}^{m(k)}\left[\hat{\boldsymbol{P}}^{h}(k|k)+\left(\hat{\boldsymbol{x}}^{h}(k|k)-\hat{\boldsymbol{x}}^{fusion}(k|k)\right)\left(\hat{\boldsymbol{x}}^{h}(k|k)-\hat{\boldsymbol{x}}^{fusion}(k|k)\right)^{T}\right]\end{cases} \tag{25}$$

where the variable $\hat{\boldsymbol{x}}^{h}(k|k)$ and $\hat{\boldsymbol{P}}^{h}(k|k)$ is the estimation result from radar s^{h} at time instant k.

relate each observation to each target respectively. Then the multi-target tracking problem can be translated into the single target tracking problem.

When targets is in the maneuvering moving, there is the calculation method of $\bar{\boldsymbol{x}}_{i}(k|k-1)$ as follows.

$$\begin{cases}\bar{\boldsymbol{x}}_{j}(k|k-1)=\sum_{h=1}^{g}\hat{\boldsymbol{x}}^{0h}(k-1|k-1)c^{j}(k-1)\\ \bar{\boldsymbol{P}}_{j}(k|k-1)\\ \quad=\sum_{h=1}^{g}\begin{bmatrix}\hat{\boldsymbol{P}}^{0h}(k-1|k-1)\\ +\left(\bar{\boldsymbol{x}}_{j}(k|k-1)-\hat{\boldsymbol{x}}^{0h}(k-1|k-1)\right)\\ \left(\bar{\boldsymbol{x}}_{j}(k|k-1)-\hat{\boldsymbol{x}}^{0h}(k-1|k-1)\right)^{T}\end{bmatrix}c^{j}(k-1)\end{cases} \tag{6}$$

where the variable $\hat{\boldsymbol{x}}^{0h}(k-1|k-1)$ and $\hat{\boldsymbol{P}}^{0j}(k-1|k-1)$ is calculated by equation (21).

The data association algorithm is shown in Table 2 in the appendix. And the data association algorithm can be applied to associate observations $\{z_1(k), z_2(k), \ldots, z_N(k)\}$ with targets. The the multiple target tracking can be inverted into singlet target tracking. Then motion states of targets can be estimated.

III. ANALYSIS ON TARGET LOSING PROBABILITY

This paper considers the combat situation whose aim of managing radars to track targets is just to keep targets not lost, corresponding to the tactical case where targets are far from our defensed center and there is no need to destroy them in reality. In another view, it is not better to obtain higher tracking accuracy. Once the positions where a target may occur are all covered by a radar beam, the target will not be lost. The relationship of a target's position distribution and a radar beam is shown in Fig.3. It is known that the estimation of a target moving state obeys the distribution $p(\hat{\boldsymbol{x}}(k))-N\left(\hat{\boldsymbol{x}}(k|k), \hat{\boldsymbol{P}}(k|k)\right)$, which can be described by the ellipse in Fig.3 (b).

The target losing probability when a radar is in the single target tracking mode can be defined as (7), shown at the

TABLE 2. Algorithm 2: Data association algorithm.

Algorithm initialization: N targets, including their moving trajectories, and N observations $\{z_1(k), z_2(k), \ldots, z_N(k)\}$ from a radar are input.

Step 1: Calculate the difference between each observation and predicted observation by the following equation:

$$\boldsymbol{l}_{ij}(k) = z_i(k) - \bar{z}_j(k \mid k-1) = z_i(k) - \boldsymbol{H}(k)\bar{\boldsymbol{x}}_j(k \mid k-1), \boldsymbol{l}_{ij}(k) \in \boldsymbol{L}_{ij}(k)_{N \times N} \tag{26}$$

where the variable $\bar{z}_j(k \mid k-1)$ is the predicted observation of target t_j; the variable $\bar{\boldsymbol{x}}_j(k \mid k-1)$ is the predicted observation of target t_j.

Step 2: Calculate the residual covariance matrixes of targets by the following equation.

$$\boldsymbol{S}_j(k) = \boldsymbol{H}(k)\bar{\boldsymbol{P}}_j(k \mid k-1)\left(\boldsymbol{H}(k)\right)^T + \boldsymbol{R}(k) \tag{27}$$

Step 3: Conduct the following calculation.
If there is $\left(\boldsymbol{l}_{ij}(k)\right)^T\left(\boldsymbol{S}_j(k)\right)^{-1}\boldsymbol{l}_{ij}(k) \le 2\ln\left[\dfrac{p_{d,i}(k)}{\left(1-p_{d,i}(k)\right)\beta\left(2\pi\right)^{\mathrm{M}/2}\sqrt{\left|\boldsymbol{S}_j(k)\right|}}\right]$, then there is $e_{ij}(k) = 1, e_{ij}(k) \in \boldsymbol{E}(k)_{N \times N}$, or there is $e_{ij}(k) = 0, e_{ij}(k) \in \boldsymbol{E}(k)_{N \times N}$. The variable $p_{d,i}(k)$ is the detection probability of the radar to observation $z_i(k)$. The variable β is the density of echoes. The variable M is the dimension of measurement.

Step 4: If there is $e_{ij}(k) = 1$, then the observation $z_i(k)$ belongs to target t_j.

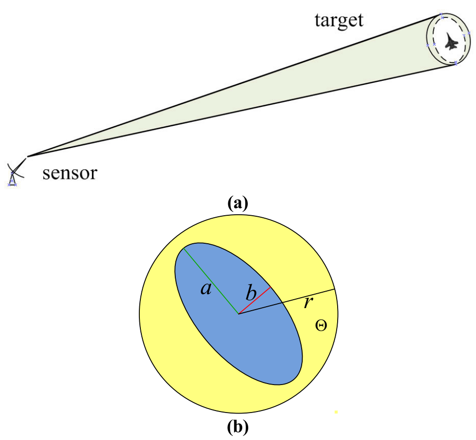

FIGURE 3. Relationship of a target's position distribution and a radar beam.

bottom of this page, where the variable Θ denotes the area covered by radar beam and is the circle in Fig.3 (b).

The radius of the radar beam can be calculated by the following equation:

$$r = 0.5\theta d \tag{8}$$

where the variable θ is the width of the radar beam and the variable d is the distance between the radar and the target.

Example 2: The target tracking accuracy is defined as $P_l = \sqrt{trace(\hat{\boldsymbol{P}}(k|k))}$, which can stand for the area of the ellipse shown in Fig.3 (b) in some degree. The relationship of target tracking accuracy and target losing probability is shown in Fig.4. It can be seen from Fig.4 that when the target moves, there is only one value for the target tracking accuracy but the target losing probability varies with the change of the radar beam's radius.

When the radar beam's radius is 400, the target losing probability keeps in a low level. When the radar beam's is less than 400, we can also reduce the target tracking accuracy by utilizing more radars to make the value of target losing probability less. It is surely becoming better when the target tracking accuracy becomes less. However, in another extent, when the target tracking accuracy is so little that the area of the ellipse is totally covered by the radar beam, there is no need to make target tracking accuracy less, even it will bring radar resource waste at this time. We just limit the ellipse into the circle in Fig.3 so that the target losing probability can be reduced to the lowest value 0 and there is no radar resource wasting.

Calculating the target losing probability through equation (7) will take more time due to integration. In target tracking, the radar beam is assumed to be focused on the position $(\hat{\boldsymbol{x}}(k|k)(1,1), \hat{\boldsymbol{x}}(k|k)(3,1))$ at time instant k so that the center of the ellipse and the circle is the same one point. We can find that once the semi-major axis a and semi-minor axis b of the ellipse in Fig.3 (b) are both less than the radius of the circle in Fig.3 (b), there will be no target losing. In order to simplify the integration, we calculate the semi-minor and semi-major axis of the ellipse instead. In fact, for the reason that the variable $\left(\hat{\boldsymbol{x}}(k|k), \hat{\boldsymbol{P}}(k|k)\right)$ can't be obtained when observations occur at time instant k, the radar beam is focused on the point $(\hat{\boldsymbol{x}}(k|k-1)(1,1), \hat{\boldsymbol{x}}(k|k-1)(3,1))$ based on the prediction $N\left(\bar{\boldsymbol{x}}(k|k-1), \bar{\boldsymbol{P}}(k|k-1)\right)$, where there is $\bar{\boldsymbol{x}}(k|k-1) = \boldsymbol{F}\hat{\boldsymbol{x}}(k-1|k-1)$ and $\hat{\boldsymbol{P}}(k|k-1) = \boldsymbol{F}\hat{\boldsymbol{P}}(k-1|k-1)\boldsymbol{F}^T$.

The relationship of the ellipse based on $N\left(\hat{\boldsymbol{x}}(k|k), \hat{\boldsymbol{P}}(k|k)\right)$, the ellipse based on $N\left(\bar{\boldsymbol{x}}(k|k-1), \bar{\boldsymbol{P}}(k|k-1)\right)$ and the radar beam is in Fig.5.

The process of the calculating $\bar{a}$ and $\bar{b}$ at time instant $k-1$ is described in Table 3 in the appendix. Algorithm 3 is used to describe the target tracking losing probability. And the tracking ellipse can be obtained through this algorithm. Its input is the target motions states $(\hat{\boldsymbol{x}}(k|k), \hat{\boldsymbol{P}}(k|k))$, and its output is the target losing probability.

$$p_{losing} = 1 - p_d(k)\iint_{\Theta}\left\{\begin{array}{l}\dfrac{1}{2\pi\sqrt{\hat{\boldsymbol{P}}(k|k)(1,1)}\sqrt{\hat{\boldsymbol{P}}(k|k)(3,3)}\sqrt{1-\hat{\boldsymbol{P}}(k|k)(1,3)}} \\ \times\exp\left\{\dfrac{-1}{2(1-\hat{\boldsymbol{P}}(k|k)(1,3))}\left[\begin{array}{l}\dfrac{(x-\hat{\boldsymbol{x}}(k|k)(1,1))^2}{\hat{\boldsymbol{P}}(k|k)(1,1)} - 2\sqrt{1-\hat{\boldsymbol{P}}(k|k)(1,3)} \\ \times\dfrac{(x-\hat{\boldsymbol{x}}(k|k)(1,1))(x-\hat{\boldsymbol{x}}(k|k)(3,1))}{\sqrt{\hat{\boldsymbol{P}}(k|k)(1,1)}\sqrt{\hat{\boldsymbol{P}}(k|k)(3,3)}} + \dfrac{(x-\hat{\boldsymbol{x}}(k|k)(3,1))^2}{\hat{\boldsymbol{P}}(k|k)(3,3)}\end{array}\right]\right\}\end{array}\right\}\mathrm{d}x\mathrm{d}y \tag{7}$$

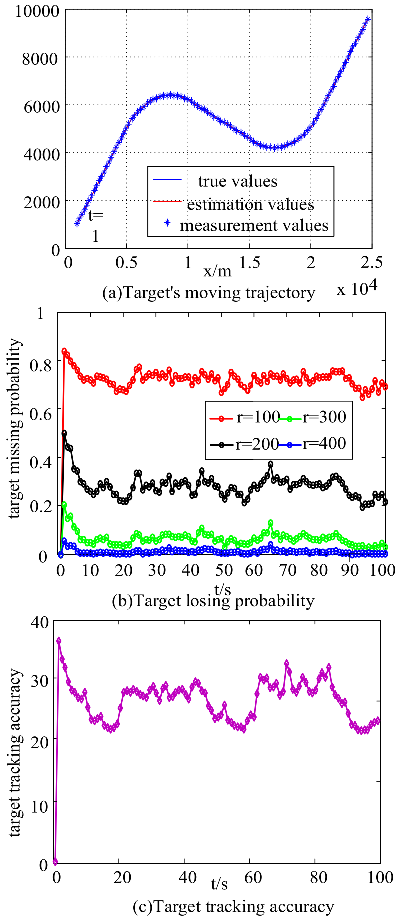

FIGURE 4. Relationship of target tracking accuracy and target losing probability.

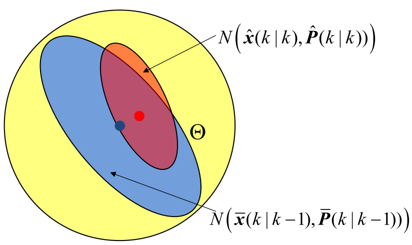

FIGURE 5. Relationship of the target motion state estimation and radar beam.

When radars are in the multi-target tracking mode, a radar beam scans all monitoring space in an observation period, and all probable occurring space of targets can be detected, then the target losing probability is just the losing alarming probability $1-p_d$. In this case, the target detection p_d for one target is much smaller than that when radars are in the single target tracking mode, for the reason that the radiation is allocated to multiple targets simultaneously.

IV. SENSOR MANAGEMENT MODELS

This section introduces radar interception probability firstly, based on which two sensor management models are built in two cases, which are sensor management in a large defending scope with the working mode 1 introduced in Section IIB

TABLE 3. Algorithm 3: The algorithm of making the ellipse.

Step 1: Calculate the predicted state $N\left(\bar{\boldsymbol{x}}(k\,|\,k-1),\bar{\boldsymbol{P}}(k\,|\,k-1)\right)$ with the result $N\left(\boldsymbol{F}\hat{\boldsymbol{x}}(k-1\,|\,k-1),\boldsymbol{F}\hat{\boldsymbol{P}}(k-1\,|\,k-1)\boldsymbol{F}^T\right)$.
Step 2: Calculate eigenvalues and eigenvectors of $\bar{\boldsymbol{P}}_1(k\,|\,k-1)$, which is a 2×2 matrix and represents the distribution of position. There is $\bar{a}=\sqrt{\lambda_1}$ and $\bar{b}=\sqrt{\lambda_2}$, where λ_1 and λ_2 are the eigenvalues of this covariance matrix. The obliquity of the ellipse is $\phi=\arctan\left(\boldsymbol{Vector}(y)/\boldsymbol{Vector}(x)\right)$, where the variable $\boldsymbol{Vector}$ is the eigenvector corresponding to the biggest eigenvalue.
Step 3: Draw the ellipse with the center $(\hat{\boldsymbol{x}}(k\,|\,k-1)(1,1),\hat{\boldsymbol{x}}(k\,|\,k-1)(3,1))$.

and sensor management in a small defending scope with the working mode 2 introduced in Section IIB.

A. RADAR EMISSION INTERCEPTION PROBABILITY

When the a radar beam is focused on a target, and radar emission is intercepted by the enemy, four conditions should be satisfied simultaneously, including power, space domain, time domain, and frequency domain. The radar radiation interception probability can be calculated by the equation $p_l = p_1p_2p_3p_4$, where p_l denotes the radar radiation interception probability, p_1 denotes the power interception probability, p_2 denotes space domain interception probability, p_3 denotes the time domain interception probability, and p_4 denotes the frequency domain interception probability.

The variable p_1 can be calculated by:

$$\begin{cases} p_1 = 0.5\mathrm{erfc}(\sqrt{-\ln p_{f_1}} - \sqrt{SNR_1 + 0.5}) \\ SNR_1 = SNR_{cal_1}(\dfrac{P\tau}{P_{cal}\tau_{cal}})(\dfrac{r}{r_{cal_1}})^{-2} \end{cases} \tag{9}$$

where p_{f_1} is the given false alarm probability; r is the distance between the target and the radar; τ is the radiation time and P is the radiation power; The variable SNR_{cal_1} is a calibrated value—the SNR of the received signal on condition that a radar radiates for τ_{cal} time with the radiation power P_{cal} and distance r_{cal_1}.

When the target is being tracked, there is $p_2 = 1$, for the reason that the radar beam focuses on the target in the whole tracking process. The time domain and the frequency domain should be combined, for the reason that scanning all frequencies of electromagnetic waves takes some time. The variable n_1 denotes the number of frequencies and n_2 denotes the number of beam positions to be scanned by the receiver. The variable t_0 denotes the time spend to scan a kind of frequency at a certain beam position. Then the total time spend to scan n_1 kinds of frequency at n_2 beam positions is $\tau_T = n_1n_2t_0$. During a period of time τ, the receiver can scan n_3 kinds of frequency, and $n_3 = \tau/t_0$. Then p_3p_4 can be calculated by:

$$p_3p_4 = \begin{cases} \dfrac{n_3}{n_1n_2} = \dfrac{\tau}{\tau_T}, & \textit{if there is } \tau < \tau_T \\ 1, & \textit{if there is } \tau \geq \tau_T \end{cases} \tag{10}$$

Above all, there is the calculation of radar emission interception probability as follows:

$$p_l = 0.5\text{erfc}(\sqrt{-\ln p_{f_1}} - \sqrt{SNR_{cal_1}(\frac{P\tau}{P_{cal}\tau_{cal}})(\frac{r}{r_{cal_1}})^{-2} + 0.5)\frac{\tau}{\tau_T} \quad (11)$$

When there are $n(k)$ targets are tracked by one radar, the joint interception probability can be calculated by:

$$p_l^*(k) = 1 - \prod_{j=1}^{n(k)} \left(1 - p_{l,j}(k)\right) \quad (12)$$

Example 3: Assume that there are $SNR_{cal_1} = 30\text{dB}$, $P_{cal} = 1kW$, $\tau_{cal} = 10ms$, $r_{cal_1} = 20km$, and $p_{f_1} = 0.01$. Then the change of radiation interception probability when the target is moving in the same simulation scene of Fig.1 can be shown as Fig.6 shows.

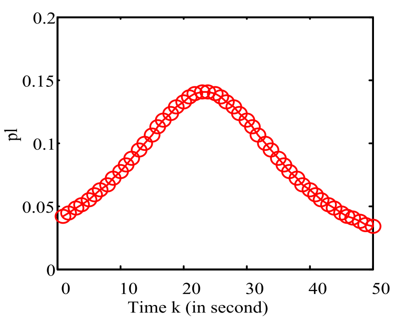

FIGURE 6. Radar radiation emission interception probability changing with time.

It can be seen that from Fig. 1, Fig.4 and Fig.6, there remains a significant inverse relationship between the indicators SNR, σ_r, σ_θ, p_d and the distance from targets to sensors. However, the indicators, including losing probability and radiation interception probability, are positively correlated with the distance.

B. SENSOR MANAGEMENT IN A LARGE DEFENDING SCOPE WITH THE SINGLE TARGET TRACKING MODE

This subsection takes the target tracking scene in a large defending scope, where pretty radars locate and targets move in a high velocity. In this case, we can select the most proper radars to satisfy the radar management objective function. When the position distributions of targets are all covered by radar beams, the target losing probability in equation (7) can be changed into $p_{los\sin g} = 1-p_d^*(k)$, where the variable $p_d^*(k)$ is the joint detection probability.

In a large defending scope, air targets keep in a high moving velocity such as hundreds of meters in a second. Radars are distributed on the ground, and their moving velocities are low such as several meters in a second. In this case, radars can't adjust their locations to keep the distances between them to targets actively, for the reason that their moving can be ignored compared with targets'. But we can choose a suitable target-radar allocation to conduct the target tracking task in radar's single target tracking mode. The different kinds of allocations are shown in Fig.7.

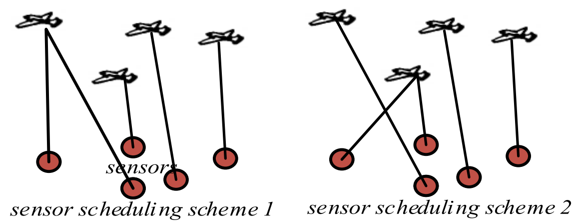

FIGURE 7. Sketch of sensor-target allocation schemes.

Denote the matrix $\boldsymbol{U}(k) = [u_{ij}(k)]_{M\times N}$, $u_{ij}(k) \in \{0, 1\}$ as radar management scheme. $u_{ij}(k) = 1$ denotes that radar s_i is used to track targets t_j, or $u_{ij}(k) = 0$ denotes not.

On the consideration that more radiation emission will result in the bigger radiation interception probability by the enemy's radiation receiver, the number of sensors in the one observation should not be too big to in case of interception. We should schedule radars as less as possible in one period of measurement, thus the optimal sensor management scheme is calculated by the following objective function.

$$\pi = \arg\left\{\min mize\left\{\begin{aligned}&\omega\sum_{i=1}^{M}\left(1-\prod_{j=1}^{N}\left(1-E\left(p_{l,ij}(k)\right)\right)^{u_{ij}(k)}\right)\\&+(1-\omega)\sum_{j=1}^{N}E\left(\sqrt{trace(\hat{\boldsymbol{P}}_j^*(k|k))}\right)\end{aligned}\right\}\right\} \quad (13)$$

where the variable $\bar{p}_{l,ij}(k)$ is the predicted interception probability by target t_j for radar s_i at time instant k; $E(\bullet)$ is the expectation calculation; ω is the weight parameter with the value $\omega = 0.995$.

subjects to: (1) Each position distribution of sensors is covered by a radar beam at least, then there is $\bar{a}_1(k) \le r, \bar{a}_2(k) \le r, .., \bar{a}_j(k) \le r, \ldots, \bar{a}_N(k) \le r$, $\bar{b}_1(k) \le r, \bar{b}_2(k) \le r, .., \bar{b}_j(k) \le r, \ldots, \bar{b}_N(k) \le r$;

(2) The joint detection probability to each target should receive the threshold value, then there is $\bar{p}_{d,1}^*(k) \ge \gamma, \bar{p}_{d,2}^*(k) \ge \gamma, \ldots, \bar{p}_{d,j}^*(k) \ge \gamma, \ldots, \bar{p}_{d,N}^*(k) \ge \gamma$;

(3) One radar can track one target at most meanwhile, and there is $\sum_{j=1}^{N} u_{ij} \le 1$.

C. SENSOR MANAGEMENT IN A SMALL DEFENDING SCOPE WITH THE MULTIPLE TARGET TRACKING MODE

This subsection considers the target tracking scene in a small defending scope, where only a few of radars distribute and targets move in a low velocity. In this case, when targets move in a low velocity such as several meters in a second, their velocities are almost the same with radars.

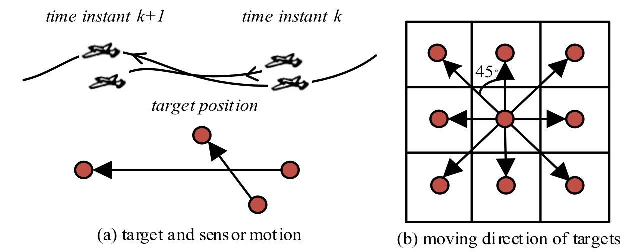

FIGURE 8. **Sketch of moving sensors as targets moves.**

Each radar can track all targets at the same time in the multiple target tracking mode. There are not too many sensors to select, however, radars can adjust their locations to improve the tracking performance. The radar moving portray and feasible moving directions are shown in Fig.8. Feasible moving direction in a time instant can be divided into the following nine choices, including keeping stable.

As Fig.8 (b) shows, assuming that the position of a radar is $(x^s(k-1), y^s(k-1))$ at time instant $k-1$, the feasible positions at time instant k can be:

$$\boldsymbol{U}(k) = \left\{ \left(x^s(k), y^s(k)\right) \in \left\{ \begin{array}{l} \left(\begin{array}{l} x^s(k-1)+v^s\Delta T\cos\left(h\dfrac{2\pi}{N_\theta}\right), \\ y^s(k-1)+v^s\Delta T\sin\left(h\dfrac{2\pi}{N_\theta}\right) \end{array} \right) \\ \cup\,(x^s(k-1), y^s(k-1)) \end{array} \right\} \right\},$$

$$N_\theta = 8, \quad h \in \{1, 2, \ldots, N_\theta\} \tag{14}$$

where the variable v^s is the velocity of radars.

The sensor management objective function is as follows:

$$\pi = \arg\left\{ \min mize \left\{ \begin{array}{l} \omega\displaystyle\sum_{i=1}^{M}\left(1-\prod_{j=1}^{N}\left(1-E\left(p_{l,ij}(k)\right)\right)\right) \\ +(1-\omega)\displaystyle\sum_{j=1}^{N}E\left(\sqrt{trace(\hat{\boldsymbol{P}}_j^*(k|k))}\right) \end{array} \right\} \right\} \tag{15}$$

subjects to:

The joint detection probability to each target should arrive at the threshold value, then there is: $\bar{p}^*_{d,1}(k) \geq \gamma, \bar{p}^*_{d,2}(k) \geq \gamma, \ldots, \bar{p}^*_{d,j}(k) \geq \gamma, \ldots, \bar{p}^*_{d,N}(k) \geq \gamma$.

There are the variable $\lambda = 0.95$.

D. DISTRIBUTED SENSOR MANAGEMENT PROCESS

The distributed sensor management process in this case can be shown as follows.

Step 1: At time instant $k-1$, each radar predicts targets motion states of the nest time instant and utilizes the sensor management objective function to produce their controlling orders, containing their moving direction;

Step 2: Radars adjust their positions obeying controlling orders;

Step 3: At time instant k, radars take observations from targets;

Step 4: Radars broadcast their observations to other radars in the network;

Step 5: Radars receive data and fuse all observations to product the estimations of target motion states.

Step 6: Set $k-1=k$, and go back to Step 1.

In this distributed sensor management process, sensors share the same information with each other, thus their calculation results remaining nearly the same.

V. SIMULATIONS

In this section, the sensor management methods proposed in this paper are simulated to claim their effectiveness, including three portions. Firstly, the compared methods with the proposed one are introduced. After that, simulations on the two sensor management methods proposed in Section IV subsection B (namely method 1) and Section V subsection C (namely method 2) are conducted.

A. THE COMPARED METHODS

In simulation, two sensor management methods are compared with the two proposed sensor management methods, and they are the sensor management based on random control (namely method 3) and sensor management based on information (namely method 4). There is no target losing probability constraint in the two latter methods.

In method 3, when radars are immovable and can only track on target mostly in a large defending scope, radars are allocated to targets randomly, and when radars are mobile and can track multiple targets simultaneously in a small defending scope, radars change their locations randomly.

In method 4, radars are allocated to targets or change their locations obeying the most information gain rule. Shannon entropy [36], [37] is usually used to describe the information amount in an event. Let $p_0 - \boldsymbol{N}(\bar{\boldsymbol{X}}(k|k-1), \bar{\boldsymbol{P}}(k|k-1))$ denote the prior probability of target t's motion state before observation and $p_1 - \boldsymbol{N}(\hat{\boldsymbol{X}}(k|k), \hat{\boldsymbol{P}}(k|k))$ denote the posterior probability of target t's motion state after a radar has fused its observation. The information gain based on Shannon entropy is as follows:

$$S(p_1||p_0) = \ln\left(\sqrt{\left\|\hat{\boldsymbol{P}}(k|k)\right\|}\Big/\sqrt{\left\|\bar{\boldsymbol{P}}(k|k-1)\right\|}\right) \tag{16}$$

Renyi entropy is the generalized form of Shannon entropy. When the probability of the random variable $\boldsymbol{X}$ changes from f_1 to f_2, its Renyi entropy is defined as:

$$\Upsilon_\alpha(f_1||f_2) = \frac{1}{\alpha-1}\ln\left(\int f_1^\alpha f_2^{1-\alpha}dx\right) \tag{17}$$

where the variable α is a parameter [38].

In target tracking, the information gain after fusing observations can be calculated by the following equation. And the

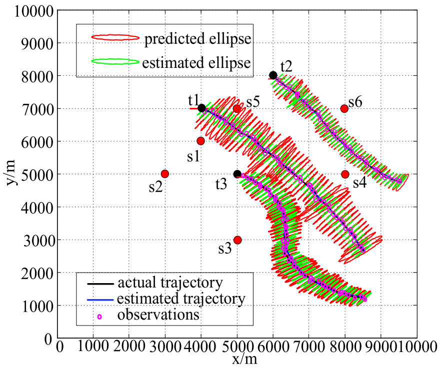

FIGURE 9. Sketch of target moving trajectories.

information gain is defined as follows.

$$\begin{aligned}
&\Upsilon_\alpha(p_1||p_0)\\
&= \frac{1}{\alpha-1}\ln\left(\int p_1^{\alpha}(x)p_2^{1-\alpha}(x)dx\right)\\
&= \frac{1}{2(\alpha-1)}\ln\frac{\left|\bar{\boldsymbol{P}}(k|k-1)\right|^{\alpha}\left|\hat{\boldsymbol{P}}(k|k)\right|^{1-\alpha}}{\left|\alpha\bar{\boldsymbol{P}}(k|k-1)+(1-\alpha)\hat{\boldsymbol{P}}(k|k)\right|}\\
&\quad -\frac{\alpha}{2}\left(\hat{\boldsymbol{X}}(k|k)-\bar{\boldsymbol{X}}(k|k-1)\right)^{T}\begin{pmatrix}\alpha\bar{\boldsymbol{P}}(k|k-1)\\+(1-\alpha)\hat{\boldsymbol{P}}(k|k)\end{pmatrix}^{-1}\\
&\quad \times\left(\hat{\boldsymbol{X}}(k|k)-\bar{\boldsymbol{X}}(k|k-1)\right)
\end{aligned} \tag{18}$$

B. SIMULATION ON MULTI-TARGET TRACKING WHEN RADARS ARE IN THE SINGLE TARGET TRACKING MODE

The initial states of four targets are

$$\boldsymbol{X}_1(0) = \begin{bmatrix}4000 & 100 & 6000 & -60 & 0\end{bmatrix}^T,$$
$$\boldsymbol{X}_2(0) = \begin{bmatrix}6000 & 100 & 8000 & -80 & 0\end{bmatrix}^T,$$

and $\boldsymbol{X}_3(0) = \begin{bmatrix}5000 & 100 & 5000 & -80 & \pi/3\end{bmatrix}^T$. The three targets move with 50 seconds in the monitoring space $\Omega_{10000\times 10000}$, where six sensors distribute with locations $s_1(4000, 6000)$, $s_2(3000, 5000)$, $s_3(5000, 3000)$, $s_4(8000, 5000)$, $s_5(5000, 7000)$ and $s_6(8000, 7000)$. The flight trajectories of targets are as Fig.10 shows.

In target tracking, three sensor management methods, including method 1, method 3 and method 4, are compared in tracking performance. When the proposed sensor management method in the constraint of target losing probability (method 1) is used to track targets, the predicted ellipses and estimated ellipses are shown in Fig.9.

It can be seen from Fig.9 that the areas of predicted ellipses are lager than those of predicted ellipses, which indicates that the tracking errors have changed to be smaller after observations are fused with predictions. In another hand, the simulation result shows that when making sensor schemes, there may be errors only according to the predicted target motion states. These sensor managements made at time instant *k-1* may not be the optimization for the motion station at time instant k.

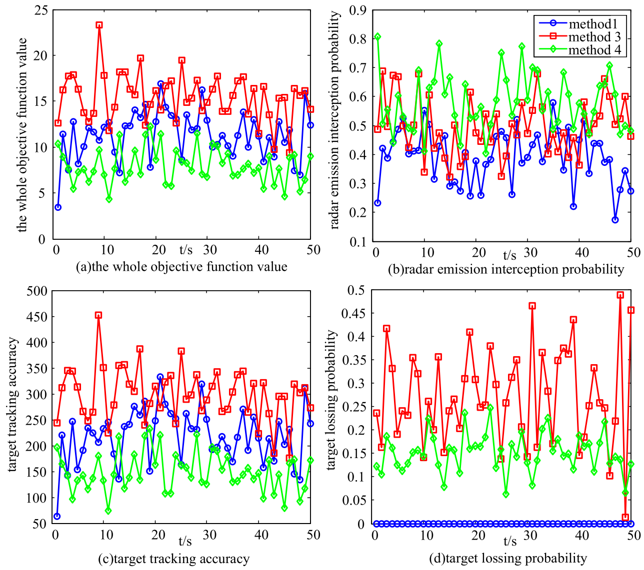

FIGURE 10. Sensor management process in case 1.

The comparison results of three sensor management methods are shown in Fig.10 and Fig.11. Fig.10(a) shows the changes of objective function values in equation (13); Fig. 10 (b) shows the changes of radar emission interception probability; Fig. 10 (c) shows the changes of target tracking accuracy; Fig.10 (d) shows the changes of target losing probability.

Fig 11(a) shows the selected sensors applied to different target using the first sensor management method at different time instants; Fig 11(b) shows the selected sensors applied to different target using the second sensor management method at different time instants; Fig 11(c) shows the selected sensors applied to different target using the third sensor management method at different time instants.

It can been seen from Fig.10(a) that the objective function values in method 4 keep almost the lowest among the three sensor management methods at most time instants, the sensor management method in the constraint of target losing probability (method 1) performs worse than the sensor management based on information gain (method 4) at most time instants, and the randomly controlling based method (method 3) behaves the worst at most time instants. The reason for this result is that for the objective function, both the target tracking accuracy and radar emission interception probability are added in method 1 as equation (13) shows. However, in method 4, only the target tracking accuracy is taken into consideration and optimized to the greatest extent. Although the radar emission probability in method 4 is greater that in method 1, the target tracking accuracy is smaller than that in method 1. Thus the sum of target tracking accuracy and radar emission interception probability is smaller than that in method 1.

It can been seen from Fig.10(b) that the radar emission interception probability values in method 1 keeps almost the lowest at most time instants, method 3 performs worse than

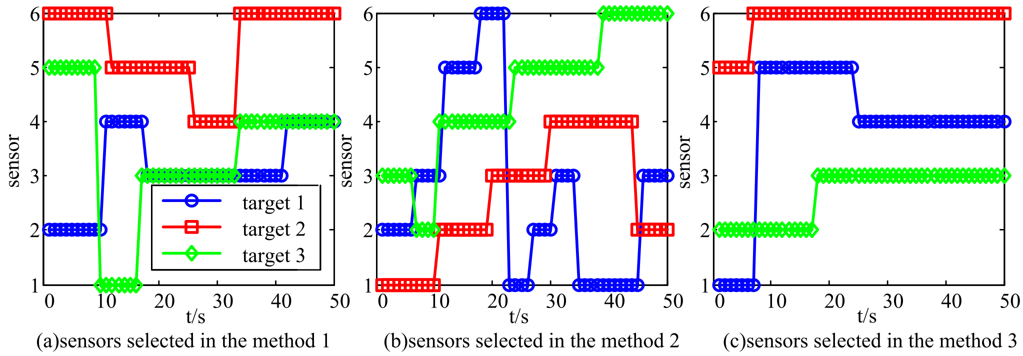

FIGURE 11. Sensor management schemes in case 1.

method 1, and method 4 behaves the worst among three sensor management methods. The reason for this result is that only in method 1, the radar emission interception probability is optimized shown as equation (13). And in method 4, more radars are used to improve the target tracking accuracy, leading to the biggest radar emission interception probability.

It can been seen from Fig.10(c) that the target tracking accuracy values in method 4 keeps almost the lowest at most time instants, method 1 performs worse than method 1, and method 3 behaves the worst among three sensor management methods. The reason for these results is that in method 4, more radars are sacrificed to achieve better target tracking performance ignoring the emission interception. And only the target tracking accuracy is optimized in method 4. In method 1, the radar emission interception probability is also optimized in the objective function. So less radars are used to track targets in order to reduce the radar emission interception probability, leading worse target tracking accuracy, but lower radar emission interception probability.

It can been seen from Fig.10(d) that the target losing probability values in method 1 keeps almost the lowest at most time instants, method 4 performs worse than method 1, and method 3 behaves the worst among three sensor management methods. The reason for this result is that only in method 4, the target losing probability is considered and optimized.

This simulation results mentioned above show that by applying the sensor management method proposed in this paper, targets cannot be easily lost and radar can be well protected at the same time. Compared with method 3, which doesn't control sensors to track targets and make sensor obtain observations randomly, method 1 and method 4 can both improve the tracking performance.

Fig.11 shows the sensor management schemes changing with time when targets move. It can be seen that in the whole target tracking, radars choose targets which are in a medium distance to keep both target losing probability and emission interception probability in a low level at the same time. Radars haven't chosen the nearest targets to obtain the least tracking errors in case of a high emission interception probability, and they also haven't selected targets in the largest distance to keep a low emission interception probability in case of worse tracking performances.

C. SIMULATION ON MULTI-TARGET TRACKING WHEN RADARS ARE IN THE MULTI-TARGET TRACKING MODE

Different from Section V subsection B, radars can track multiple targets at the same time, form which we can see that the focus in sensor management is not to calculate the sensor-target allocation schemes, but to adjust the positions of radars to improve the tracking performance. This section compares performances of method 2, method 3 and method 4 in target tracking. The initial states of four targets are $\boldsymbol{X}_1(0) = \left[\,500\ 6\ 500\ -6\,\right]^T$, $\boldsymbol{X}_2(0) = \left[\,600\ 6\ 500\ 3\,\right]^T$, and $\boldsymbol{X}_3(0) = \left[\,300\ 8\ 800\ -8\,\right]^T$. The initial positions of two sensors are respectively $s_1(0) = (500, 600)$ and $s_1(0) = (500, 300)$. Fig 12 shows the moving trajectories of targets, including predicted ellipses and estimated ellipses by using method 2. What's more, the moving trajectories of two radars can also be shown in Fig.12.

When the distance from targets and sensors is small, there is perfect tracking performance with a high SNR. But in this case, the radar emission interception probability is terrible. When the distance is far, the result is inverse. In target tracking, radars can adjust their positions not only to obtain a pretty low target losing probability, but also to keep a low emission interception probability to keep themselves safe at the same time. So radars keep medium distances from targets, where they can obtain both a low target losing probability and a low emission interception probability in the whole tracking process.

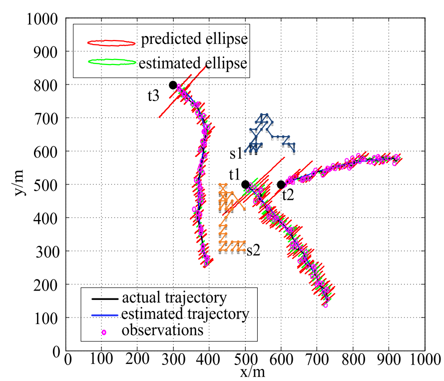

FIGURE 12. Sketch of target moving trajectories.

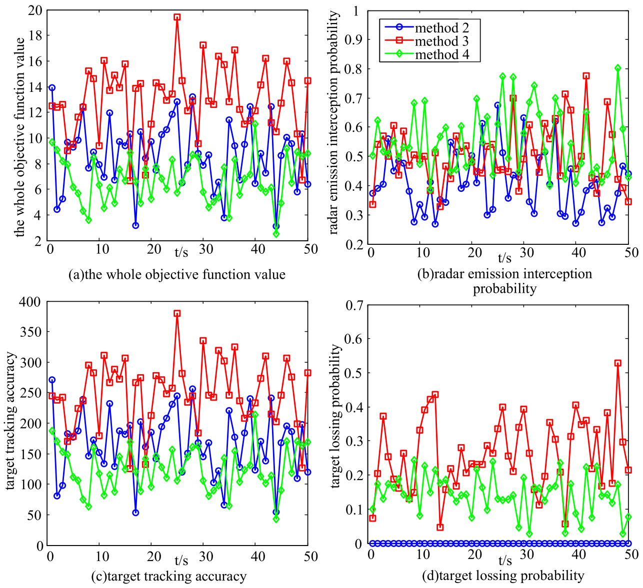

FIGURE 13. **Sensor management process in case 2.**

It can also be seen from Fig.12 that the areas of predicted ellipses are lager than those of predicted ellipses, which indicates that the tracking errors have changed to be smaller after observations are fused with predictions.

The comparison results of method 2, method 3 and method 4 are shown in Fig.13.

Fig.13(a) shows the changes of objective function values in equation (13); Fig.13 (b) shows the changes of radar emission interception probability; Fig.13 (c) shows the changes of target tracking accuracy; Fig.13 (d) shows the changes of target losing probability.

It can been seen from Fig.13(a) that the objective function values in method 4 keep almost the lowest among the three sensor management methods at most time instants, the sensor management method in the constraint of target losing probability (method 1) performs worse than the sensor management based on information gain (method 4) at most time instants, and the randomly controlling based method (method 3) behaves the worst at most time instants. The reason for this result is that for the objective function, both the target tracking accuracy and radar emission interception probability are added in method 1 as equation (13) shows. However, in method 4, only the target tracking accuracy is taken into consideration and optimized to the greatest extent. Although the radar emission probability in method 4 is greater that in method 1, the target tracking accuracy is smaller than that in method 1. Thus the sum of target tracking accuracy and radar emission interception probability is smaller than that in method 1.

It can been seen from Fig.13(b) that the radar emission interception probability values in method 1 keeps almost the lowest at most time instants, method 3 performs worse than method 1, and method 4 behaves the worst among three sensor management methods. The reason for this result is that only in method 1, the radar emission interception probability is optimized shown as equation (13). And in method 4, more radars are used to improve the target tracking accuracy, leading to the biggest radar emission interception probability.

It can been seen from Fig.13(c) that the target tracking accuracy values in method 4 keeps almost the lowest at most time instants, method 1 performs worse than method 1, and method 3 behaves the worst among three sensor management methods. The reason for these results is that in method 4, more radars are sacrificed to achieve better target tracking performance ignoring the emission interception. And only the target tracking accuracy is optimized in method 4. In method 1, the radar emission interception probability is also optimized in the objective function. So less radars are used to track targets in order to reduce the radar emission interception probability, leading worse target tracking accuracy, but lower radar emission interception probability.

It can been seen from Fig.13(d) that the target losing probability values in method 1 keeps almost the lowest at most time instants, method 4 performs worse than method 1, and method 3 behaves the worst among three sensor management methods. The reason for this result is that only in method 4, the target losing probability is considered and optimized.

This simulation results show that by applying the sensor management method proposed in this paper, targets cannot be easily lost and radar can be well protected at the same time. Compared with method 3, which doesn't control sensors to track targets and make sensor obtain observations randomly, method 2 and method 4 can both improve the tracking performance.

VI. CONCLUSION

This paper proposed a sensor management method in the constraint of target losing probability for maneuvering target tracking. Three main contributions existed in this paper. Firstly, the emission interception risk of radars was considered and added to the sensor management objective function, which should not be ignored for the reason that hostile targets could intercept our emission to find out the positions of sensors and they could further launch missiles to destroy our sensors. Secondly, two actual working modes of radars were analyzed, and they were focusing one radar beam on one target's position and scanning all directions using one radar beam, based on which the tracking performances were different. The last but not the least was to add the target losing probability to the constraints of the sensor management objective function in order to save radar resources and reduce the emission interception probability. Based on the introduction mentioned above, two sensor management models, containing sensor management in a large defending scope with the single target tracking mode and sensor management in a small defending scope with the multiple target tracking mode, were built. What's more, the distributed sensor management process was also introduced. Simulation results showed the effectiveness of the proposed sensor management method. Due to these cautions, the proposed sensor management method can keep radars in a low emission level, take different actions when radars are in different working modes, and avoid sensor resource from being wasted. Besides these advantages, there are also two shortcomings in the proposed method. The first one is that the caution of reducing emission may meaningless when the number of targets are so large that radar resources are saturated and run out of. In this case, all radars should emit radiation uninterruptedly. The second one is that regarding the target losing probability as the objective function of sensor management may lead to a poor target tracking accuracy. This is not allowed when missiles are launched to destroy targets. In the future, the proposed sensor management methods will be improved to adjust to different target tracking scenes. And the different importance of radars in a network will be considered, based on which, we can protect radar of more importance at the sacrifice of radars of less importance.

APPENDIX

A. IMM ALGORITHM

IMM is used to estimate the motion states of maneuvering targets. After observations from sensors are obtained, they can be fused with the predicted target motion states by IMM to update the target motion states. The motion states of all possible motion models should be calculated firstly, then they are fused to make the final target motion states. The calculation process is shown in Table 1.

B. DATA ASSOCIATION ALGORITHM

Data association algorithm is used to allocate different observations with different targets respectively.

C. THE ALGORITHM OF MAKING THE ELLIPSE

It is difficult to calculate the target losing probability due to much calculation. This method provide an estimation method of target losing probability and can replace the calculation of target losing probability. The calculation is as follows.

REFERENCES

[1] C. Qiao, G. Shan, L. Yan, and X. Duan, "Nonmyopic sensor scheduling for target tracking with emission control," *Int. J. Adapt. Control Signal Process.*, vol. 33, no. 5, pp. 767–783, May 2019.
[2] M. Marcos, A. N. Vasconcelos, and M. Urbashi, "Optimal sensor management strategies in networked estimation," in *Proc. IEEE 56th Annu. Conf. Decis. Control*, Melbourne, VIC, Australia, Dec. 2017, pp. 5378–5385.
[3] J. J. Guo and C. Z. Han, "A novel sensor selection approach with Bayes framework for target tracking," *Chin. J. Automat.*, vol. 44, no. 8, pp. 1425–1435, 2018.
[4] O. M. Bushnaq, A. Chaaban, S. P. Chepuri, G. Leus, and T. Y. Al-Naffouri, "Sensor placement and resource allocation for energy harvesting IOT networks," *Digit. Signal Process.*, early access, Jan. 21, 2020, doi: 10.1016/j.dsp.2020.102659.
[5] I. Tkach and Y. Edan, "Multi-sensor task allocation systems," in *Distributed Heterogeneous Multi Sensor Task Allocation Systems* (Automation, Collaboration, & E-Services), vol. 7. Cham, Switzerland: Springer, 2010.
[6] J. Guerreiro, L. Rodrigues, and N. Correia, "Resource allocation model for sensor clouds under the sensing as a service paradigm," *Computers*, vol. 8, no. 1, p. 18, Feb. 2019.
[7] I. Tkach, A. Jevtić, S. Nof, and Y. Edan, "A modified distributed bees algorithm for multi-sensor task allocation," *Sensors*, vol. 18, no. 3, p. 759, Mar. 2018.
[8] J. Wang, J. Qin, Q. Ma, Y. Kang, and X. Fu, "Optimal sensor scheduling for two linear dynamical systems under limited resources in sensor networks," *Neurocomputing*, vol. 273, pp. 101–110, Jan. 2018.
[9] K. Li, C. Yuen, B. Kusy, R. Jurdak, A. Ignjatovic, S. S. Kanhere, and S. Jha, "Fair scheduling for data collection in mobile sensor networks with energy harvesting," *IEEE Trans. Mobile Comput.*, vol. 18, no. 6, pp. 1274–1287, Jun. 2019.
[10] X. Gao, Z. Chen, J. Pan, F. Wu, and G. Chen, "Energy efficient scheduling algorithms for sweep coverage in mobile sensor networks," *IEEE Trans. Mobile Comput.*, vol. 19, no. 6, pp. 1332–1345, Jun. 2020.
[11] X. Gongguo, S. Ganlin, and D. Xiusheng, "Non-myopic scheduling method of mobile sensors for manoeuvring target tracking," *IET Radar, Sonar Navigat.*, vol. 13, no. 11, pp. 1899–1908, Nov. 2019.
[12] J. Wang, J. Tang, G. Xue, and D. Yang, "Towards energy-efficient task scheduling on smartphones in mobile crowd sensing systems," *Comput. Netw.*, vol. 115, pp. 100–109, Mar. 2017.
[13] R. B. Diddigi, K. J. Prabuchandran, and S. Bhatnagar, "Novel sensor scheduling scheme for intruder tracking in energy efficient sensor networks," *IEEE Wireless Commun. Lett.*, vol. 7, no. 5, pp. 712–715, Oct. 2018.
[14] J. Xu, C. Wen, Q. Ge, and D. Xu, "Optimal multiple-sensor scheduling for general scalar Gauss–Markov systems with the terminal error," *Syst. Control Lett.*, vol. 108, pp. 1–7, Oct. 2017.
[15] M. Yigit, P. S. Boluk, and V. C. Gungor, "A new efficient error control algorithm for wireless sensor networks in smart grid," *Comput. Standards Interfaces*, vol. 63, pp. 27–42, Mar. 2019.
[16] Y. Tao and H. Chongzhao, "Sensor management for multi-target detection and tracking based on PCRLB," in *Proc. 20th Int. Conf. Inf. Fusion (Fusion)*, Xi'an, China, Jul. 2017, pp. 1–6.
[17] S. Joshi and S. Boyd, "Sensor selection via convex optimization," *IEEE Trans. Signal Process.*, vol. 57, no. 2, pp. 451–462, Feb. 2009.
[18] G. G. Xu, C. Pang, X. Duan, and G. Shan, "Multi-sensor optimization scheduling for target tracking based on PCRLB and a novel intercept probability factor," *Electronics*, vol. 8, no. 2, pp. 140–162, 2019.
[19] H. G. Hong, B.-N. Vo, B.-T. Vo, and R. Mahler, "The Cauchy–Schwarz divergence for Poisson point process," *IEEE Trans. Aerosp. Electron. Syst.*, vol. 61, no. 8, pp. 4475–4485, Aug. 2015.
[20] R. Tharmarasa, T. Kirubarajan, A. Sinha, and T. Lang, "Decentralized sensor selection for large-scale multisensor-multitarget tracking," *IEEE Trans. Aerosp. Electron. Syst.*, vol. 47, no. 2, pp. 1307–1324, Apr. 2011.
[21] G. Ferri, A. Munafo, and K. D. LePage, "An autonomous underwater vehicle data-driven control strategy for target tracking," *IEEE J. Ocean. Eng.*, vol. 43, no. 2, pp. 323–343, Apr. 2018.
[22] M. Bukal, I. Markovic, and I. Petrovic, "Score matching based assumed density filtering with the von Mises-Fisher distribution," in *Proc. 20th Int. Conf. Inf. Fusion (Fusion)*, Xi'an, China, Jul. 2017, pp. 433–438.
[23] M. O. Sayin, C. W. Lin, J. Shen, T. Basar, and S. Shiraishi, "Information-driven autonomous intersection control via incentive compatible mechanisms," *IEEE Trans. Intell. Transp. Syst.*, vol. 20, no. 3, pp. 912–914, Mar. 2019.
[24] H. Chen, Z. L. He, and B. Liu, "Sensor control method based on information entropy measure for multi-target tracking," *Chin. J. Control Decis.*, vol. 33, no. 2, pp. 337–344, 2018.
[25] C. Hui, H. Zhongliang, L. Feng, and L. Chen, "Threat assessment based sensor control for multi-target tracking," *J. Electron. Inf. Technol.*, vol. 40, no. 12, pp. 2861–2867, 2018.
[26] A. K. Gostar, R. Hoseinnezhad, and A. Bab-Hadiashar, "Multi-Bernoulli sensor-selection for multi-target tracking with unknown clutter and detection profiles," *Signal Process.*, vol. 119, pp. 28–42, Feb. 2016.
[27] A. K. Gostar, R. Hoseinnezhad, T. Rathnayake, X. Wang, and A. Bab-Hadiashar, "Constrained sensor control for labeled multi-Bernoulli filter using Cauchy-Schwarz divergence," *IEEE Signal Process. Lett.*, vol. 24, no. 9, pp. 1313–1317, Sep. 2017.
[28] A. A. Kadri, I. Kacem, and K. Labadi, "A branch-and-bound algorithm for solving the static rebalancing problem in bicycle-sharing systems," *Comput. Ind. Eng.*, vol. 95, pp. 41–52, May 2016.
[29] O. Ozturk, M. A. Begen, and G. S. Zaric, "A branch and bound algorithm for scheduling unit size jobs on parallel batching machines to minimize makespan," *Int. J. Prod. Res.*, vol. 55, no. 6, pp. 1815–1831, Mar. 2017.
[30] S.-J. Yoo, A. P. Shrestha, M. Seo, C.-H. Han, M. Park, and K.-E. Lee, "Joint spectrum sensing and resource allocation optimization using genetic algorithm for frequency hopping-based cognitive radio networks," *Int. J. Commun. Syst.*, vol. 31, no. 13, p. e3733, Sep. 2018.

[31] Z. Lyu, Z. Wei, J. Pan, H. Chen, C. Xia, J. Han, and L. Shi, "Periodic charging planning for a mobile WCE in wireless rechargeable sensor networks based on hybrid PSO and GA algorithm," *Appl. Soft Comput.*, vol. 75, pp. 388–403, Feb. 2019.
[32] N. Bogdanovic, H. Driessen, and A. G. Yarovoy, "Target selection for tracking in multifunction radar networks: Nash and correlated equilibria," *IEEE Trans. Aerosp. Electron. Syst.*, vol. 54, no. 5, pp. 2448–2462, Oct. 2018.
[33] Z. H. Tian, X. S. Gao, S. Su, J. Qiu, X. J. Du, and M. Guizani, "Evaluating reputation management schemes of Internet of vehicles based on evolutionary game theory," *IEEE Trans. Veh. Technol.*, vol. 68, no. 6, pp. 5971–5980, Jun. 2019.
[34] A. S. Narkov and A. Yarovoy, "Sensor selection algorithm for optimal management of the tracking capability in multisensor radar system," in *Proc. 10th Eur. Radar Conf.*, Nuremberg, Germany, Oct. 2013, pp. 499–502.
[35] B. R. Mahafza, *Radar Systems Analysis and Design Using MATLAB*. Beijing, China: Publishing House Electronic Industry, 2008, pp. 201–231.
[36] S. Mishra and M. B. Ayyub, "Shannon entropy for quantifying uncertainty and risk in economic disparity," *Electronics*, vol. 39, no. 10, pp. 2160–2181, 2019.
[37] H. Zenil, S. Hernández-Orozco, N. Kiani, F. Soler-Toscano, A. Rueda-Toicen, and J. Tegnér, "A decomposition method for global evaluation of Shannon entropy and local estimations of algorithmic complexity," *Entropy*, vol. 20, no. 8, p. 605, Aug. 2018.
[38] Y. Liu, H. Wang, and C. Hou, "UKF based nonlinear filtering using minimum entropy criterion," *IEEE Trans. Signal Process.*, vol. 61, no. 20, pp. 4988–4999, Oct. 2013.

GANLIN SHAN is currently a Professor with the Shijiazhuang Campus of Army Engineering University, China. His research interests include intelligent information processing and sensor management.

CE PANG is currently pursuing the Ph.D. degree with the Shijiazhuang Campus of Army Engineering University, China. His research interest includes information.